Solid-state time-gated luminescence microscope with ultraviolet light-emitting diode excitation and electron-multiplying charge-coupled device detection

Russell Connally
James Piper
Macquarie University
Centre for Laser Applications
Sydney, Australia 2109

Abstract. Many naturally occurring materials are autofluorescent, a property that can reduce the discriminative ability of fluorescence methods, sometimes to the point where they cannot be usefully applied. Shifting from the spectral to the temporal domain, it is possible to discriminate fluorophores on the basis of their fluorescence decay lifetime. Luminophores with sufficiently long lifetimes can be discriminated from short-lived autofluorescence using time-gated luminescence (TGL). This technique relies upon the application of a brief excitation pulse followed by a resolving period to permit short-lived autofluorescence to decay, after which detection is enabled to capture persistent emission. In our studies, a high-power UV LED was mounted in the filter capsule of an Olympus BX51 microscope to serve as the excitation source. The microscope was fitted with an Andor DV885 electron-multiplying CCD (EM-CCD) camera with the trigger input synchronized to UV LED operation. *Giardia lamblia* cysts labeled with the europium chelate BHHST were analyzed against an autofluorescent background with the TGL microscope. The EM-CCD camera captured useful TGL images in real time with a single exposure cycle. With 4x frame averaging, images acquired in TGL mode showed a 30-fold improvement in SNR compared with conventional fluorescence microscopy.
[DOI: 10.1117/1.2928169]

Keywords: time-gated luminescence; UV LED; europium; chelate; lanthanides; Giardia lamblia; autofluorescence.

Paper 07472R received Nov. 25, 2007; revised manuscript received Jan. 15, 2008; accepted for publication Jan. 15, 2008; published online May 19, 2008.

1 Introduction

Many naturally occurring substances are autofluorescent when excited with UV or visible wavelengths. Autofluorescence emission typically spans the visible spectrum with a lifetime (τ) measured in nanoseconds. One of the earliest reports of using a probe fluorescence lifetime (τ) to discriminate against nonspecific background autofluorescence was made by Thaer and Sernetz in 1973.[1] Since then, a number of microscopes with the ability to resolve different fluorophores on the basis of τ have been reported.[2–5] Instruments that operate in the time domain to resolve fluorophores that differ in τ by a large degree (ns versus μs) have the advantage of simplicity and lower cost compared to microscopes required to resolve fluorophores on the basis of a few nanoseconds' difference. The time-gated luminescence (TGL) microscope described here operates within the time domain to capture long-lived (greater than 100 μs) emission after autofluorescence has decayed. Figure 1 illustrates the basic concept of TGL; with the detector off, the TGL cycle begins with a short, powerful excitation pulse that raises the target luminophore into its excited state. On termination of the excitation pulse, nonspecific fluorescence decays rapidly while target luminescence persists for orders of magnitude longer. After a resolving period (gate delay), the detector is gated on (acquisition period) to capture luminescent emission in the absence of autofluorescence.

TGL microscopes employ a pulsed excitation scheme at a wavelength suited to the target luminophore. Platinum and palladium porphyrin based luminophores can be excited at either 390 or 540 nm; a number of solid-state or semiconductor excitation sources are suitable for this role. Unlike the former compounds, lanthanide chelates are not oxygen sensitive and can provide longer lifetimes (0.5 to 2 ms). They are normally employed with the ions bound to a sensitizer molecule to boost the absorbance cross-section. Typically they require excitation in the UV region of the spectrum (Tb^{3+}: 320 nm; Eu^{3+}: 337 nm), with the upper useful limit being about 370 nm for terpyridine-based europium chelates (~15% effective at 337 nm). Some europium chelates in novel configurations can be excited at longer wavelengths (365 to 400 nm), although they were not used for this work due to other important limitations.[6–9] The luminescence life-

Address all correspondence to Russell Connally, Physics Department, Division of Information & Communication Sciences, Macquarie University, Balaclava Road, Sydney, NSW 2109 Australia; Tel: +61 2 9850 8111; Fax: +61 2 9850 8115; E-mail: rconnall@ics.mq.edu.au

1083-3668/2008/13(3)/034022/6/$25.00 © 2008 SPIE

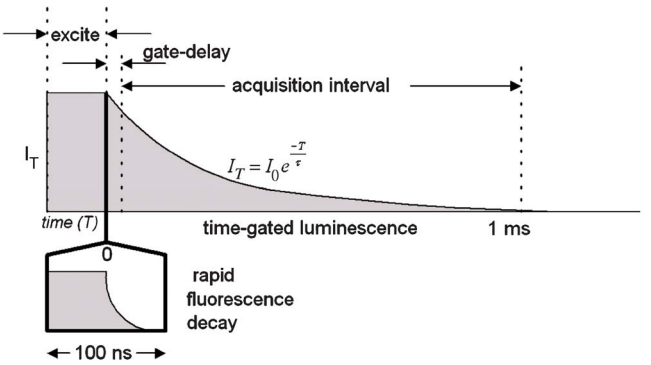

Fig. 1 TGL suppresses autofluorescence by delaying signal acquisition until prompt (auto-fluorescence) has faded. Lanthanide chelate luminescence can persist for milliseconds, greatly facilitating its detection in the absence of autofluorescence.

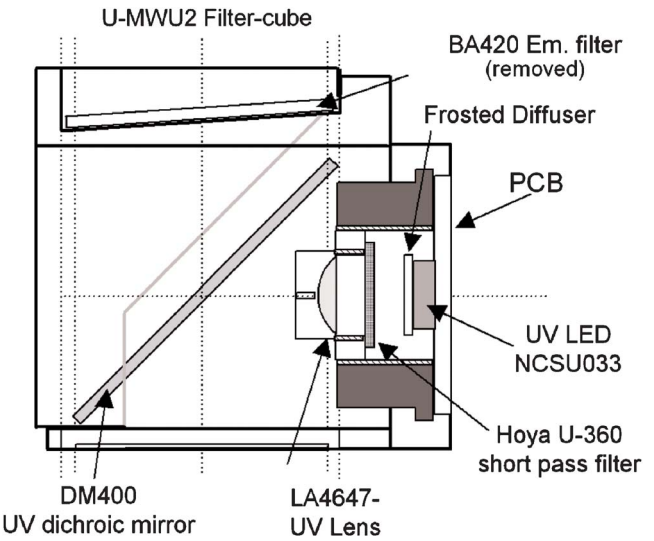

Fig. 2 Cutaway view of the U-MWU2 Olympus filter cube illustrating the optical components of the Nichia NCSU033 UV LED excitation scheme. Due to the narrow passband of the LED emission, both the excitation and emission filters were removed from the filter assembly for this work.

time of europium chelates is typically around 300 to 600 μs in aqueous environments and follows single exponential decay kinetics.

Microscopes designed for use with lanthanide chelates usually employ pulsed UV sources such as Xe flashlamps, or nitrogen-laser or chopper-interrupted Hg arc lamps.[10–15] As a consequence of their low duty cycle, phosphors emit relatively weakly compared with most fluorophores and therefore require sensitive detectors. All previously reported TGL microscopes have required multiple excitation detection cycles to deliver an image of acceptable contrast and quality. The detector integrates photons over many TGL cycles, and it is necessary to shield the sensor from light during the excitation cycle. Microchannel-plate image intensifiers that employ electronic gating are used to satisfy this requirement, whereas conventional CCD cameras require an external shutter mechanism. Regardless of the technique used, multiple excitation cycles have been necessary, requiring either an expensive gated image intensifier,[11,14–21] a vibration-prone mechanical beam interruptor (chopper),[12,22] or a high-insertion-loss ferroelectric LCD shutter[14,20] to control the light reaching the detector.

We previously reported the design of a UV LED-excited TGL microscope for use with europium fluorophores.[23] The recent availability of electron-multiplying CCD (EM-CCD) cameras prompted us to consider their application in TGL microscopy. EM-CCD cameras are the solid-state equivalent of image-intensified CCD cameras, albeit with lower gain, which is compensated to some extent by a threefold improvement in quantum sensitivity.

While EM-CCD cameras offer high sensitivity, they still require an external shutter mechanism if multiple TGL cycles are to be employed for each acquisition. Alternatively, if a single exposure cycle is sufficient, as with the system described here, the shutter can be eliminated.

2 Method

2.1 *UV LED*

Due to the small size of the LED, the device was mounted within an Olympus U-MWU2 filter cube as shown in Fig. 2. The UV LED (NCSU033A, Nichia Corp., Japan) used for this work was an improved device rated at 220 mW (365 nm) at 500 mA, about double the output power of the previous version (NCCU033). The LED was surface-mounted to a 25-mm-diameter single-sided printed circuit board (PCB) that replaced the excitation filter in the cube. In the confined space of the cube, it was not possible to achieve Koehler illumination and a diffuser (frosted glass slide) was mounted on the front face of the LED to homogenize the beam. To the eye, the excitation region appeared uniform in intensity, although scatter from the diffuser was estimated to reduce output power by about 15%. Power was supplied to the LED via flexible power leads that entered the filter housing at its central axis to permit filter cubes on either side of the UV LED to be rotated into view. The filter housing was thus limited to rotation ± 60 deg from the UV LED axis due to the length of the power leads.

Earlier we reported the existence of low-intensity self-excited visible luminescence from InGaN-based LEDs that persists for some time following switch-off and that can present a problem when the devices are used in pulse fluorometry applications.[24,25] To suppress this component, a short-pass filter (Hoya U-360, Edmund Optics, Singapore) was included in the excitation beam path that was situated about 3 mm from the LED face, as shown in Fig. 2. A fused silica lens $\phi = 12.7$ mm, f.l = 20 mm (LA4647-UV, Thorlabs, Newton, New Jersey) was mounted approximately 16 mm from the LED face to collimate the excitation radiation. The filtered excitation beam was then directed into the microscope objective via the DM400 dichroic mirror. This mirror strongly reflects wavelengths below 380 nm while transmitting visible (>400 nm) light better than 90%. The increased optical clarity of this arrangement helped maximize fluorescence and excitation efficiency of the instrument.

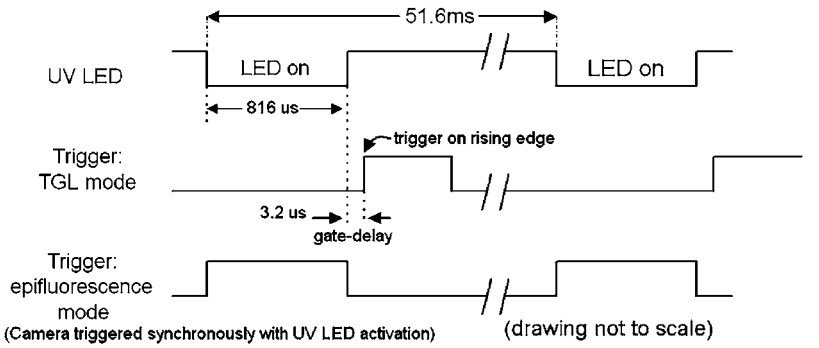

Fig. 3 Pulse timing for the UV LED and camera trigger pulse when operated in conventional epifluorescence mode (prompt). While this mode of operation uses a pulsed source, it appears continuous to the camera and eye, returning conventional fluorescence images. Rise time of the LED pulse on turn-off was 1.33 V/μs; the camera was triggered about 3.2 μs after the LED pulse. This small gate-delay resulted in a loss of about 1% of the initial intensity of the europium label at the moment of acquisition.

2.2 *Instrumentation*

An Olympus BX51 fluorescence microscope was used for this work, and images were acquired without the benefit of spectral filtering. The UV-LED was supplied from a programmable voltage source so that it could be driven at two different power levels. The LED current was monitored by measuring the peak voltage across the 5-ohm LED load resistor with an oscilloscope; in low-power mode, the current was 288 mA at a supply voltage of 5.5 V, and in high-power mode, it was 1.44 amps at 11.6 V. The LED was always operated in pulsed mode, and it was convenient to switch to low-power mode to limit photobleaching when higher-duty cycles or long observation periods were employed.

2.3 *LED Output Power*

A Coherent FieldMax™ -TO laser power meter fitted with a model PS10Q detector head was used for power measurements. The output face of the U-MWU2 filter cube was fixed approximately 2 cm from the PS10Q sensor for power measurements. The pulse profile for both the TGL and epifluorescence modes is shown in Fig. 3. The rising edge of the trigger pulse would shift from the start to the end of the UV LED pulse when it was switched from prompt (epifluorescence) mode to TGL mode. The duration of the LED pulse was 816 μs with a 51.6-ms resting period between each pulse, corresponding to a frequency of 19.38 Hz and a duty cycle of 1:63. The observed average power was 370 μW with a calculated peak power of 23.4 mW. In idle mode (volts =5.5 V), the observed average power was 105 μW with a calculated peak power of 6.64 mW. The LED (still fitted with the diffuser) was then removed from the filter cube and placed 2 cm from the sensor. In TGL mode, the average power reading was 1.205 mW with a peak power of 76.2 mW, or 3.05-fold higher than when mounted in the cube. In idle mode, the average power was 275 μW with a 17.4-mW peak power, corresponding to 2.6 times thepower level when mounted in the cube.

By comparison, our previously reported UV-LED filter assembly, which lacked both the diffuser and the Hoya 360 filter, delivered an average power of 470 μW with a 29.72-mW peak (LED in filter cube) when measured with the FieldMax™ power meter.[23]

2.4 *EM-CCD Camera*

An iXon DV885 EM-CCD was fitted to the microscope using a standard C-mount lens adaptor. The DV885 camera specifications include: Texas Instruments 1004×1002 Impactron frame transfer CCD sensor, 8×8 μm pixels, EM gain 2000, quantum efficiency of 65% at 600 nm, 14-bit digitized output, 24 full frames per second, and external trigger mode support. An embedded microcontroller was used to control the camera, which was operated in "fast external trigger" mode so the instrument could be switched instantly between conventional "prompt" fluorescence and TGL modes. To make the system more versatile, a microcontroller was used to control the gate-delay interval, repetition frequency, trigger pulse polarity, LED pulse length, and drive intensity parameters. In fast-trigger mode the sensor and its registers are cleared pending the arrival of the trigger pulse, the rising edge of which initiates frame capture within nanoseconds. A gate delay of 3.2 μs was imposed between the termination of the LED pulse and the rising edge of the trigger pulse.

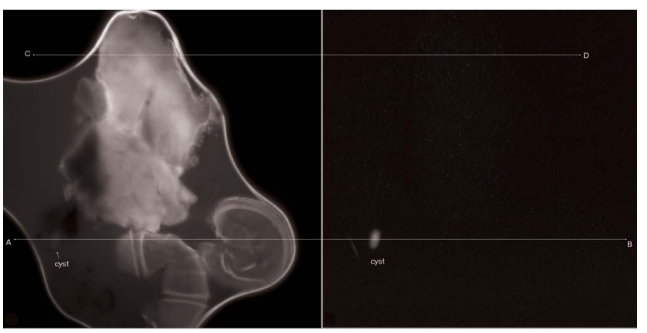

Fig. 4 Line A-B transects a BHHST-labeled *Giardia* cyst that was (a) captured in conventional epifluorescence mode and (b) acquired in TGL mode. The cyst in this instance was encountered within an island of fluid containing the fluorescent dye DMACA together with autofluorescent debris from the water concentrate. A bright region of autofluorescence was sampled along the second line profile C-D and compared with the same region captured in TGL mode.

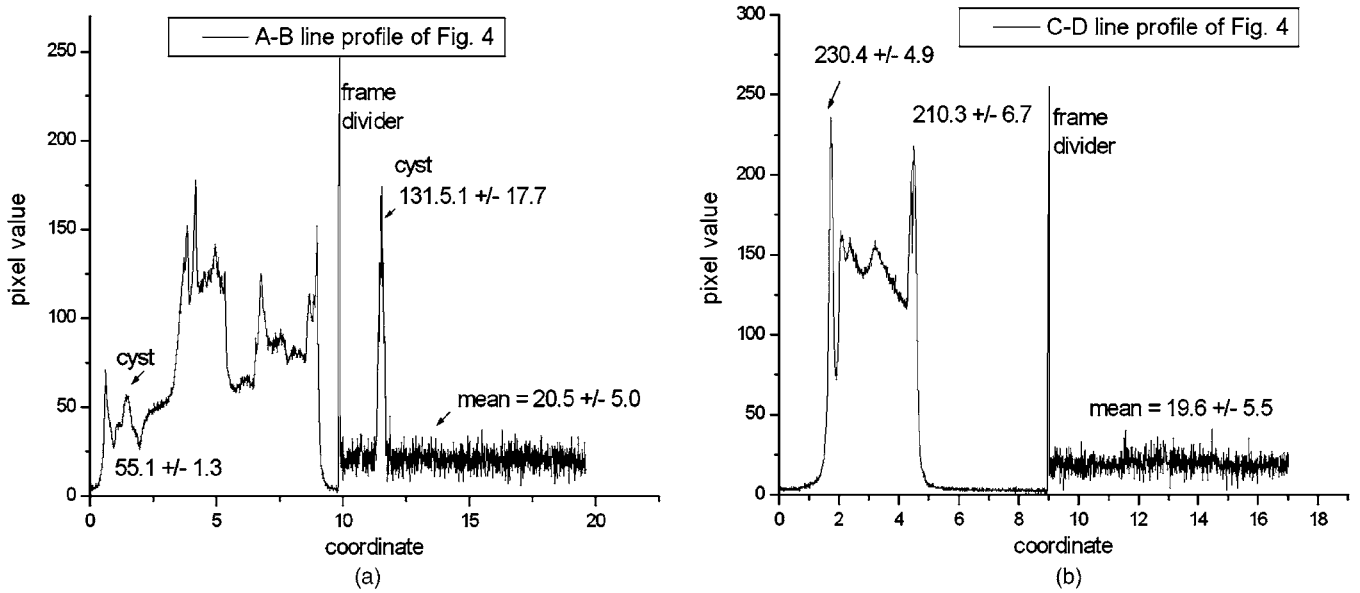

Fig. 5 (a) Line profile A-B was sampled to compare pixel values on the labeled cyst for prompt and TGL modes. (b) Second line profile C-D in Fig. 4 transits a strongly fluorescent region that was used to determine the effectiveness of TGL suppression. Data from both regions was used to calculate the improvement in SNR (30-fold).

2.5 *Test Sample*

Giardia lamblia cysts (Biotech Frontiers Pty. Ltd., Sydney, Australia) were labeled using the europium chelate BHHST (4,4′-bis-(1″,1″,1″,2″,2″,3″,3″-heptafluoro-4″,6″-hexanedion-6″-yl) sulfonyl-aminopropyl-ester-N-succinimide-ester-*o*-terphenyl), the synthesis and use of which has previously been reported.[26] The 10,000:1 concentrate isolated from the Sydney water supply used for this work was a kind gift from Dr. Belinda Ferrari and was prepared from 10 L backwash water samples using the flocculation method.[27] To further increase the autofluorescence background, the UV excitable fluorophore 7-dimethylaminocoumarin-4-acetic acid (DMACA) was added to the water concentrate together with the *Giardia* cysts.

3 Results and Discussion

The addition of DMACA resulted in strong background fluorescence that limited visibility of the *Giardia* cyst situated at the bottom-left of Fig. 4(a). This 8-bit image was acquired using a 40× objective, a 3-ms exposure with averaging enabled (4 x frames), and EM gain turned off. Figure 4(b) was acquired after the microscope was switched to TGL mode and EM gain was increased to 1185. The line A-B transects the cyst in both the prompt and TGL capture frames to generate the profile shown in Fig. 5(a). For background determination, the second line profile C-D was sampled; pixel values for this trajectory are shown in Fig. 5(b). Data points from these two sets were analyzed to determine the effective improvement in the signal-to-noise ratio (SNR), and key values used for this calculation are shown in Table 1. The SNR figures were based on the average 8-bit intensity value of the cyst referenced to the brightest region of nonspecific fluorescence within the frame. In prompt epifluorescence mode, the cyst emitted weakly in comparison with other regions and a SNR of 0.23 ± 0.012 was obtained. In TGL mode, the cyst was the only object visible and the SNR improved 30-fold to a value of 7.04 ± 2.58. The relatively large error bars arise from the small sample size of 17 (for the cyst) with pixel values ranging from 104 to 174.

3.1 *Effect of Frame Averaging*

Software supplied with the iXon camera provided the option to average successive frames and improve image quality

Table 1 Summary of the input values used to calculate the improvement in SNR for the *Giardia* cyst shown in Fig. 4. To compare Figs. 4(a) and 4(b), the SNR was determined by sampling identical regions and calculating the ratio of the brightest signal to the brightest (autofluorescent) background. The effective improvement was taken as the ratio of TGL_{SNR} to $PROMPT_{SNR}$.

Mode	Prompt				TGL			
Region	Average	SD	*n*	SNR	Average	SD	*n*	SNR
Cyst	54.5	1.74	9	0.23±.012	131.5	17.7	17	7.04±2.58
Background	230.4	4.9	5		20.5	5.0	601	

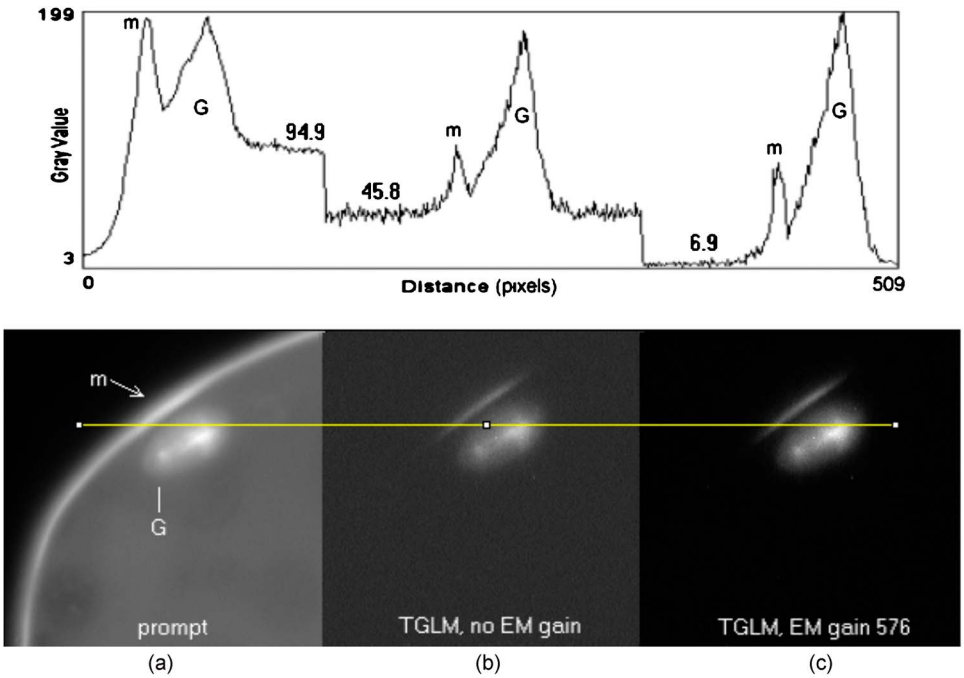

Fig. 6 A BHHST-labeled *Giardia* cyst (labeled G) suspended in an aqueous solution of DMACA was captured in (a) conventional epifluorescence mode, (b) TGL mode without the assistance of EM-gain, and (c) TGL mode with EM-gain enabled. The line profile shown above the sequence illustrates graphically the reduction in background that was achieved in each of these modes. SNR was improved progressively from 1 to 4.6 to 28 in Fig. 6(c). The arc-shaped region to the left of the cyst in Figs. 6(b) and 6(c) arises from cyst luminescence reflected by the liquid meniscus (m) as the DMACA solution evaporated.

through reduction of random noise components. Averaging significantly improved the SNR by decreasing the background noise level. For example, a background region (sample count=15,104 pixels) within a single frame acquired under TGL conditions had an average value of 21.58 ± 4.78. When the same frame was averaged over four successive frames, the background dropped to 12.97 ± 2.59. Increasing the frame count to 8 resulted in a further small improvement in SNR (about 7%).

The improvement in signal strength achieved by frame averaging was determined by monitoring an oval region (sample count=532 pixels) on a *Giardia* cyst present within the frames captured for background measurements. The mean pixel value for the region after a single acquisition was 163.1 ± 28.96, and this was improved to 177.7 ± 28.91 when four successive frames were averaged (data not shown).

3.2 *EM Gain and its Effect on SNR*

BHHST is a strongly luminescent europium chelate that was conjugated to the anti-*Giardia* monoclonal antibody G203 for the detection of *Giardia lamblia* cysts. The iXon camera employs a very sensitive sensor, and it was possible to capture images of well-labeled *Giardia* cysts even without the assistance of EM gain. Figure 6(a) was captured in conventional epifluorescent mode and shows an image of a *Giardia* cyst suspended within a background of fluorescent DMACA. The line profile at the top reports pixel intensity from left to right across the three frames [6(a) to 6(c)], and the fluid meniscus and center of the cyst have roughly equal (peak) pixel intensities. Figure 6(b) was captured in TGL mode with EM gain turned off. Referring again to the line profile, it is apparent that fluorescence from the DMACA was strongly suppressed, and the SNR improved from an initial value of about 1 to 4.6. The crescent at the top of the cyst was an artifact arising from scattered luminescence focused by the meniscus. EM gain (576) was enabled to acquire the image shown in Fig. 6(c) that had significantly reduced background levels compared with Figs. 6(a) and 6(b). The SNR for this image was improved to around 28 (199/7) by virtue of background suppression and signal strength enhancement delivered by the camera with EM gain enabled.

Our results support the conclusion that substantial improvements in SNR can be achieved in TGL mode without a shutter when EM gain and frame averaging are employed. Increased optical throughput to detector, decreased instrument complexity, and finer control of the gate-delay interval (to maximize detection efficiency) are key benefits arising from the elimination of the shutter.

4 Conclusion

The solid-state instrument described here implemented a short gate-delay to capture target luminescence at maximal intensity. Good image quality was achieved after a single excitation cycle of 800 μs when camera EM gain was enabled. While the excitation and exposure portion of a TGL cycle are essentially complete after 4 ms, the acquisition process must be extended to 40 ms to allow for the frame readout time. This interval is still faster than the time taken for a motorized stage to ramp up to speed, move to a new location, and stabilize.

An important feature of TGL techniques is the reduction in image complexity that facilitates the use of computer recognition systems to process images for the identification of target organisms based on their morphology. We intend to investigate these techniques for the automated detection of methicillin-resistant *Staphylococcus Aureus* (MRSA) in sputum samples.

For TGL microscopy, the introduction of inexpensive solid-state LED excitation sources was an exciting development, and the recent availability of EM cameras was equally significant. The cost of implementing TGL microscopy has plummeted while image resolution, SNR, and acquisition rates have improved greatly. With solid-state instrumentation, we believe that TGL microscopy has finally come of age.

Acknowledgments

We wish to thank the Australian Research Council (ARC) and Olympus Australia for their generous assistance and support under the ARC Linkage Program (LP0775196).

References

1. A. A. Thaer and M. Sernitz, "Fluorescence techniques in cell biology," in *Proc. of a conference held at the Battelle Seattle Research Center, Seattle, Washington, March 27–31, 1972*, Springer-Verlag, Berlin, 420 pp (1973).
2. G. Bottiroli, "Time resolved fluorescence microscopy: a new tool in chromatin study," *Basic Appl. Histochem.* **25**(4), 297–302 (1981).
3. G. Marriott, R. M. Clegg, D. J. Arndt-Jovin, and T. M. Jovin, "Time resolved imaging microscopy. Phosphorescence and delayed fluorescence imaging," *Biophys. J.* **60**(6), 1374–1387 (1991).
4. J. Gadella, W. J. Theodorus, T. M. Jovin, and R. M. Clegg, "Fluorescence lifetime imaging microscopy (FLIM): Spatial resolution of microstructures on the nanosecond time scale," *Biophys. Chem.* **48**(2), 221–239 (1993).
5. M. Rulli, A. Kuusisto, J. Salo, H. Kojola, and O. Simell, "Time-resolved fluorescence imaging in islet cell autoantibody quantitation," *J. Immunol. Methods* **208**, 169–179 (1997).
6. J. Wu, G. Wang, D. Jin, J. Yuan, Y. Guan, and J. Piper, "Luminescent europium nanoparticles with a wide excitation range from UV to visible light for biolabeling and time-gated luminescence bioimaging," *Chem. Commun. (Cambridge)* **3**, 365–367 (2008).
7. R. Pal and D. Parker, "A single component ratiometric pH probe with long wavelength excitation of europium emission," *Chem. Commun. (Cambridge)* **5**, 474–476 (2007).
8. A. Dadabhoy, S. Faulkner, and P. G. Sammes, "Long wavelength sensitizers for europium(III) luminescence based on acridone derivatives," *J. Chem. Soc., Perkin Trans. 2* **2**, 348–357 (2002).
9. R. C. Leif, L. M. Vallarino, M. C. Becker, and S. Yang, "Increasing the luminescence of lanthanide complexes," *Cytometry* **69A**(8), 767–778 (2006).
10. H. B. Beverloo, A. van Schadewijk, S. van Gelderen-Boele, and H. J. Tanke, "Inorganic phosphors as new luminescent labels for immunocytochemistry and time-resolved microscopy," *Cytometry* **11**(7), 784–792 (1990).
11. B. D. Venetta, "Microscope phase fluorimeter for determining the fluorescence lifetimes of fluorochromes," *Rev. Sci. Instrum.* **30**, 450–457 (1959).
12. L. Seveus, M. Vaisala, S. Syrjanen, M. Sandberg, A. Kuusisto, R. Harju, J. Salo, I. Hemmila, H. Kojola, and E. Soini, "Time-resolved fluorescence imaging of europium chelate label in immunohistochemistry and *in-situ* hybridization," *Cytometry* **13**(4), 329–338 (1992).
13. H. B. Beverloo, A. van Schadewijk, J. Bonnet, R. van der Geest, R. Runia, N. P. Verwoerd, J. Vrolijk, J. S. Ploem, and H. J. Tanke, "Preparation and microscopic visualization of multicolor luminescent immunophosphors," *Cytometry* **13**(6), 561–570 (1992).
14. N. P. Verwoerd, E. J. Hennink, J. Bonnet, C. R. van der Geest, and H. J. Tanke, "Use of ferro-electric liquid crystal shutters for time-resolved fluorescence microscopy," *Cytometry* **16**(2), 113–117 (1994).
15. T. Gadella, J. Goedhart, A. van Hoek, and A. Visser, "Construction and applications of a frequency-domain fluorescence lifetime imaging microscope," *Prog. Biophys. Mol. Biol.* **65**(Supplement 1), 92 (1996).
16. R. Connally, D. Veal, and J. Piper, "Flashlamp excited time-resolved fluorescence microscope suppresses autofluorescence in water concentrates to deliver 11-fold increase in signal to noise ratio," *J. Biomed. Opt.* **9**(4), 725–734 (2004).
17. R. J. Hennink, R. de Haas, N. P. Verwoerd, and H. J. Tanke, "Evaluation of a time-resolved fluorescence microscope using a phosphorescent Pt-porphine model system," *Cytometry* **24**, 312–320 (1996).
18. A. A. Zotikov and Y. S. Polyakov, "The use of the phosphorescence microscope for the study of the phosphorescence of various cells," *Microsc. Acta* **79**(5), 415–418 (1977).
19. A. S. Verkman, M. Armijo, and K. Fushimi, "Construction and evaluation of a frequency-domain epifluorescence microscope for lifetime and anisotropy decay measurements in subcellular domains," *Biophys. Chem.* **40**(1), 117–125 (1991).
20. R. de Haas, R. P. M. van Gijlswijk, E. B. van der Tol, H. J. M. A. A. Zijlmans, T. Bakker-Schut, J. Bonnet, N. P. Verwoerd, and H. J. Tanke, "Platinum porphyrins as phosphorescent label for time-resolved microscopy," *J. Histochem. Cytochem.* **45**(9), 1279–1292 (1997).
21. K. Hanaoka, K. Kikuchi, S. Kobayashi, and T. Nagano, "Time-resolved long-lived luminescence imaging method employing luminescent lanthanide probes with a new microscopy system," *J. Am. Chem. Soc.* **129**(44), 13502–13509 (2007).
22. N. P. Verwoerd, E. J. Hennink, J. Bonnet, C. R. G. van der Geest, and H. J. Tanke, "Use of ferro-electric liquid crystal shutters for time-resolved fluorescence microscopy," *Cytometry* **16**, 113–117 (1994).
23. R. E. Connally, D. A. Veal, and J. Piper, "High intensity solid-state UV source for time-gated luminescence microscopy," *Cytometry* **69A**, 1020–1027 (2006).
24. D. Jin, R. Connally, and J. Piper, "Ultrasensitive time-resolved nanoliter volume fluorometry based on UV LEDs and a channel photomultiplier tube," *Proc. SPIE* **5699**, 237–245 (2005).
25. D. Jin, R. Connally, and J. Piper, "Long-lived visible luminescence of UV LEDs and impact on LED excited time-resolved fluorescence applications," *J. Phys. D* **39**, 461–465 (2006).
26. R. E. Connally, D. A. Veal, and J. Piper, "Time-resolved fluorescence microscopy using an improved europium chelate BHHST for the in-situ detection of *Cryptosporidium* and *Giardia*," *Microsc. Res. Tech.* **64**, 312–322 (2004).
27. G. Vesey, J. S. Slade, M. Byrne, K. Shepherd, and C. R. Fricker, "A new method for the concentration of *Cryptosporidium* oocysts from water," *J. Appl. Bacteriol.* **75**(1), 82–86 (1993).